PRELIMINARY LONGITUDINAL IMPEDANCE MODEL FOR THE ESRF-EBS

S. White, European Synchrotron Radiation Facility, Grenoble, France

Abstract

In light sources, longitudinal beam coupling impedance can deteriorate performance through bunch lengthening or increased longitudinal emittance due to the microwave instability. Simulation estimates are therefore required to devise the appropriate counter-measures if necessary. The main contributors to the longitudinal impedance model of the new ESRF-EBS storage ring were simulated. A preliminary longitudinal impedance model is presented and preliminary tracking simulations are shown.

INTRODUCTION

The ESRF-EBS upgrade program consists of replacing the existing lattice by an **H**ybrid **M**ulti-**B**end **A**chromat (HMBA)to achieve an emittance reduction form 4000 pm to 132 pm [1, 2]. In order to achieve the required gradients all the vacuum vessels besides straight sections have to be replaced with smaller aperture chambers. This has an impact on the global machine impedance and the design of critical devices such as flanges or RF fingers. Electromagnetic simulations were performed using either CST particle studio [3] or GDFIDL [4] to minimize the geometrical impedance contribution of various devices and build the global impedance model of the machine. Tracking simulation using **A**ccelerator **T**oolbox (AT) [5] were used to estimate bunch lengthening and instability thresholds.

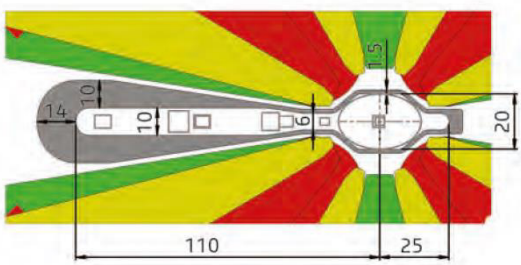

Figure 1: Chamber profile of the large aperture arc.

VACUUM VESSELS PROFILES

The ESRF storage ring is made out of 32 cells, 2 cells are dedicated to injection. Each cell can be divided into 3 distinct aperture profiles: the straight section with a full vertical aperture of 8mm (no in-vacuum undulator) the large aperture arc with a full vertical aperture of 20mm and small aperture arc with a full vertical aperture of 13 mm. The small aperture arc is required to accommodate high-gradient quadrupoles, see [1, 2] for details. Figure 1 shows the chamber profile of the large aperture arc and how it fits inside the magnets poles. The small aperture arc features the same characteristics with smaller vertical aperture while the straight section chamber has an elliptical profile. The large volume (ante-chamber) on the outer part of the ring (left on the plot) allows to transport the photons to the downstream absorber where they are stopped. Except for the change in vertical aperture and straight section chambers, electrical continuity is ensured by keeping the chamber profile constant up to ±25 mm from the beam axis over the whole ring.

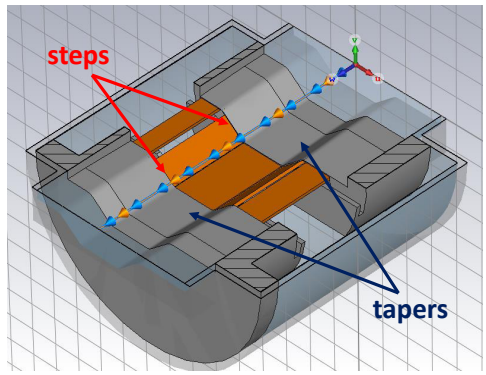

Figure 2: RF fingers design for the ESRF-EBS machine.

RF FINGERS AND FLANGES

Due to their large number of occurrences around the ring RF fingers and flanges can significantly contribute to the overall impedance of the machine. Special attention was therefore taken to minimize the impedance of these devices.

Figure 2 shows the new RF fingers design produced for the ESRF-EBS machine [6]. The RF fingers consist of a total of 10 copper blades (5 up and 5 down). The blades spacing and horizontal extension (±25mm from the beam axis) were optimized to avoid cross-talk with the bellows cavity. The fingers are held in place by aluminium pieces and thermal expansion is absorbed by sliding the fingers into these pieces providing good mechanical tightness. The geometrical impedance is then strictly defined by the inner volume and dominated by the entrance and exit tapers and steps to transition from these aluminium pieces to the the RF fingers. Figure 3 shows the reduction of longitudinal impedance after optimization of the tapers angle and geometry. The loss factor of the structure is reduced by a factor 4. A similar design is adopted for chambers with low vertical aperture, transition to insertion devices, collimators and ce-

ISBN 978-3-95450-182-3

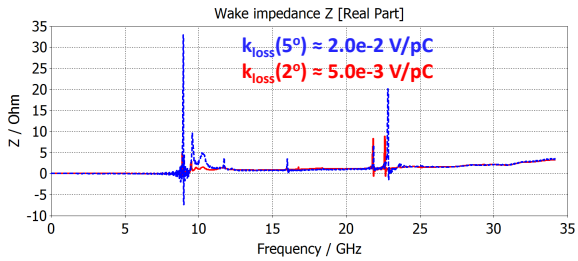

Figure 3: Optimization of the tapers impedance of ESRF-EBS RF fingers.

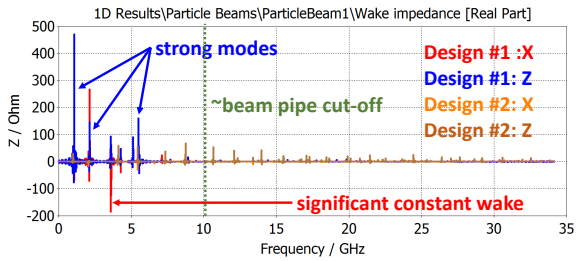

Figure 5: Zero impedance flanges sealed with aluminium gaskets and optimization of the gasket shape.

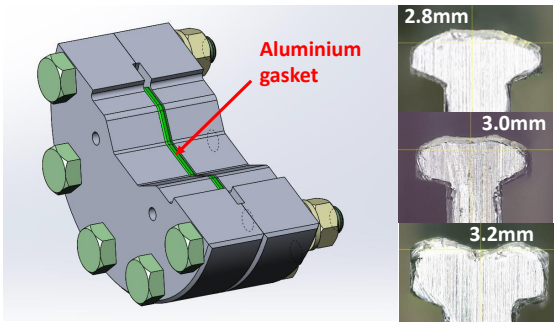

Figure 4: Impedance of the flanges of the present machine adapted to the new vacuum chambers.

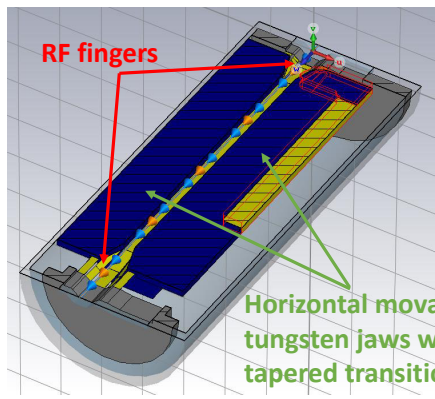

Figure 6: Top view of the ESRF-EBS collimators.

ramic chambers. Tests with beam are ongoing on the present machine.

The present flange design features a gap of approximately 0.1 mm on the beam path driving significant trapped modes below the beam pipe cut-off frequency. Two possible adaptations to the new vacuum chambers were initially proposed featuring similar gap. Figure 4 shows the result of impedance simulations for the flanges of the present machine adapted to the new chamber profile. It is seen that strong modes are present below the cut-off frequency and due to asymmetries of the chamber profile (ante-chamber) a constant horizontal wake is exited for both proposed designs. In view of these results it was decided to adopt a flat sealed flange design as proposed in [7]. Figure 5 show a view of the ESRF-EBS flanges [6]. The gap is sealed by an aluminium gasket providing perfect electrical continuity and essentially zero geometrical impedance. The gasket shape was carefully optimized to provide the best possible flatness. Examples of different shapes trial are shown on the right side of Fig. 5.

TAPERED TRANSITIONS

Tapered transitions are a major contributor to the overall longitudinal impedance. A design rule that was imposed from the beginning to the mechanical engineers was to have no angles large than 5^o. This was respected in most cases and much smaller angles could be achieved for the transitions between the large chamber profiles and the small chamber profiles where the angle is less than 1^o. However the transitions to in-vacuum undulators, RF section and collimators feature larger angles. Cooling had to be added to the RF section tapers and although the transition into in-vacuum undulators could be significantly improved by a reduction of the vertical aperture of the upstream and downstream chambers their contribution remains significant when they are either closed or fully open. In-vacuum undulators are cooled as well and no over-heating is expected in this area.

Figure 6 shows a top view of the ESRF-EBS collimators [8]. They consist of 2 movable horizontal tungsten jaws that will intercept off-momentum Touschek particles to localize losses and minimize radiation damages on critical devices such as in-vacuum undulators [9]. Besides the

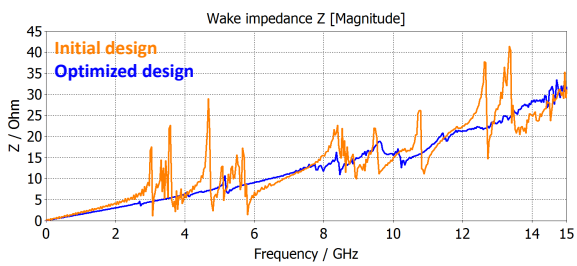

Figure 7: Impedance optimization of the ESRF-EBS collimators.

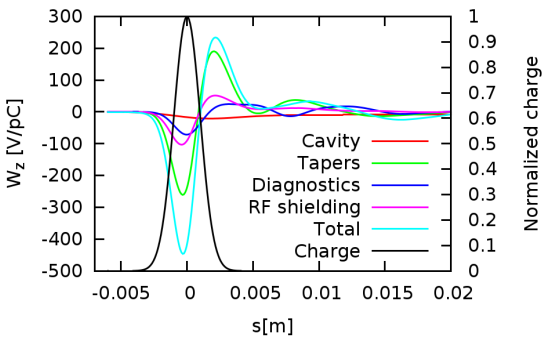

Figure 8: Impedance model with 1 mm pulse length.

obvious resistive wall contribution due to the reduction of horizontal aperture, the transition from and to the tungsten jaws had to be carefully designed in order to minimize the impedance of these devices. Figure 7 shows the longitudinal impedance of the ESRF-EBS collimators before and after optimization. All resonances are suppressed and we are left with an almost purely inductive impedance driven by the tapered transition. These could not be improved due to space limitation in the collimators area.

GLOBAL IMPEDANCE MODEL

The short-range impedance model for single-bunch computation was derived using GDFIDL [4]. Three pulse lengths were used (3mm, 2mm and 1mm) with a mesh size of at least $\sigma/10$ and in most cases $\sigma/30$ to perform convergence tests. 1 mm is the smallest bunch length allowing for affordable computation duration and memory usage on the ESRF cluster. In the specific case of RF cavity, the smallest bunch length is 2 mm due to its very large volume. The model presently includes the following elements:

- RF fingers (shielded bellows) and flanges
- Tapers (RF section, straight section and transition from small to large profile)
- Collimators and absorbers
- RF Cavities
- In-vacuum undulators (in the open position)
- Ceramic chambers with dedicated short bellows
- Horizontal and vertical striplines
- Current transformers
- Sector valves

It should be noted that pumping ports are located in the ante-chambers and their contribution to the model is therefore negligible.

Figure 8 shows the different contributions to the longitudinal short-range wake field for a bunch length of 1mm. The main contributors are tapered transitions and the geometrical impedance is therefore mainly inductive. In addition to the geometrical impedance, the resistive wall contribution is computed using the analytical code ImpedanceWake2D [10].

Figure 9 shows the tracking simulation results using AT for the different pulse length used in GDFIDL and a comparison to the most recent measurements. One can see that even for the shortest bunch length (zero current) the model is converging for 1 mm pulse length. Comparing the measured impedance to the simulation one can estimate a reduction of about a factor 2, down to 0.35 Ω, of the longitudinal impedance for the new machine which results in a shorter bunch length. The microwave threshold is however reduced from about 4 to 4.5 mA today to approximately 3.5 mA which is not critical for machine operation.

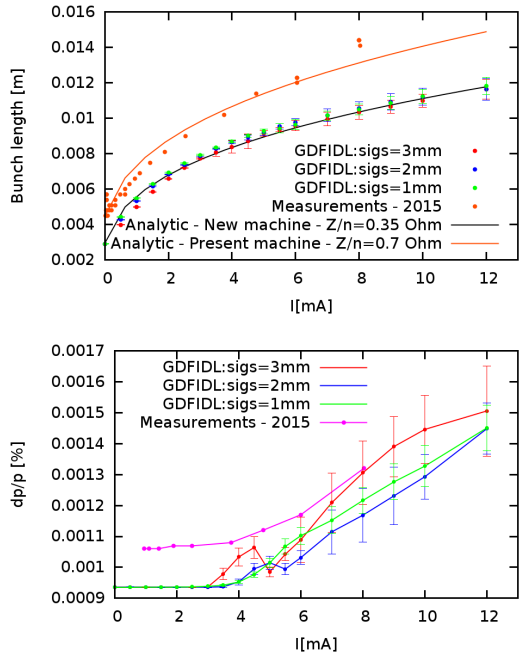

Figure 9: Simulated bunch lengthening and microwave threshold of the ESRF-EBS machine.

SUMMARY

The impedance model of the ESRF-EBS storage ring was built using GDFIDL. The main contributors to the global impedance of the machine have been included after minimization of the geometrical impedance. First tracking results indicate a reduction of a factor 2 of the longitudinal impedance with respect to the present machine. While the expected bunch length will be reduced, the microwave threshold is slightly degraded. This degradation is however not critical for the operation of the machine.

REFERENCES

[1] J.C. Biasci et al., "A low emittance lattice for the ESRF", Synchrotron Radiation News, vol. 27, Iss.6, 2014.

[2] "ESRF upgrade programme phase II", ESRF, December 2014.

[3] CST, `http://www.cst.com`

[4] GDFIDL, `http://www.gdfidl.de`

[5] A. Terebilo, "Accelerator Toolbox for MATLAB",SLAC-PUB-8732,2001.

[6] Designed by T. Brochard and P. Brummund, ESRF.

[7] H. Matsumoto et al.,"Experience with a zero impedance vacuum flange at He super-leak temperatures for the ILC",EPAC'06, Edinburgh ,MOPLS085, p. 753.

[8] Designed by J. Borrel, ESRF.

[9] R. Versteegen et al.,"Collimation scheme for the ESRF upgrade",IPAC'15, Richmond, TUPWA017,p. 1434.

[10] N. Mounet, "The LHC Transverse Coupled-Bunch Instability", EPFL PhD Thesis 5305, 2012.